

Ghost image behavior in Wolter type I x-ray telescopes

Edward C. Moran and James E. Harvey

In Wolter type I grazing incidence telescopes, ghost images result whenever unreflected x rays or singly reflected x rays pass through the telescope and impinge on the focal plane. These ghost images degrade image quality and can be eliminated by appropriately positioned stops and baffles. However, conflicting demands can be placed on an aperture design by requirements for field of view, vignetting, and ghost image control. These problems are particularly severe for high energy x-ray telescopes which require very small grazing angles of incidence. We have developed and used analytical and numerical tools to perform parametric analyses of ghost image behavior and to obtain an aperture plate design capability that can be utilized to satisfy specific ghost image requirements.

I. Introduction

Images are formed in Wolter I grazing incidence telescopes^{1,2} by x rays which reflect from both the primary and secondary mirrors. Ghost images result from any x rays which reach the focal plane unreflected or singly reflected from just one of the elements, as illustrated in Fig. 1. Because of the extreme grazing angles of the Wolter I optics, ghost images are, to an extent, unavoidable. However, ghost images often appear so far from the on-axis image position and any focal plane instrumentation that they are of no concern. When ghost images do come close to the on-axis focal point, they can seriously degrade the quality of the desired image and must be controlled.

The placement of aperture plates in the Wolter I system is, in general, the solution to the ghost image problem. Aperture plates are usually required in a Wolter I system for the structural purpose of holding the cylindrical optics together. As baffles, aperture plates limit the field of view and restrict rays that are not doubly reflected image rays. In the ghost image context, there are five functionally independent positions for aperture plates: the fore, fore intermediate, central, rear intermediate, and rear positions, as shown in Fig. 2.³ In each of these positions, the aperture plate (consisting of an annular aperture with inner

radius r_1 and outer radius r_2) plays a unique role in ghost image control. Before aperture plates can be incorporated into a Wolter I system, it is necessary to establish some criteria for their placement with respect to other telescope design parameters.

In addition to usual sensitivity and resolution requirements (e.g., effective area and encircled energy), a telescope design may also specify requirements for field of view, vignetting, and ghost image control. A vignetting requirement specifies that portion of the field of view which is to be unobstructed by any stops or baffles. A ghost image requirement specifies some minimum system ghost image performance criterion which can vary in definition but ultimately involves keeping ghost rays a safe distance from the on-axis focal point. Thus, a vignetting requirement imposes a lower bound to the size of an aperture at a given position (the aperture must be large enough to not vignette the desired field of view), and a ghost image requirement imposes an upper bound to the size of the same aperture (it must be small enough to effectively block nonimage x rays). For a particular aperture plate configuration, the situation could exist where these two bounds do not overlap, that is, where the lower bound on the aperture size imposed by the vignetting requirement is larger than the upper bound allowed by the ghost image requirement. In this way, these two requirements can place conflicting demands on the aperture plate design.

Ghost images are not a new concern to grazing incidence optics³⁻⁵; however, their effect on the optical performance of Wolter I x-ray telescopes is gaining importance as investigators in x-ray astronomy seek greater efficiency at the higher x-ray energies and require smaller grazing angles for these telescopes. It

The authors are with Perkin-Elmer Corporation, 100 Wooster Heights Road, Danbury, Connecticut 06810.

Received 1 December 1987.

0003-6935/88/081486-06\$02.00/0.

© 1988 Optical Society of America.

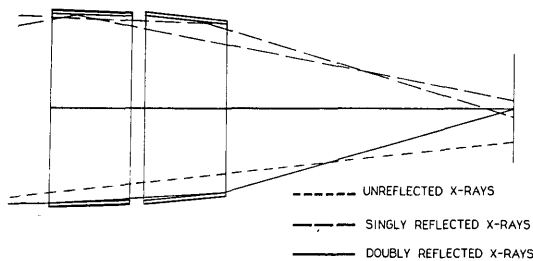


Fig. 1. Ghost images in Wolter I telescopes originate from rays which reach the focal plane unreflected or singly reflected and can seriously degrade image quality.

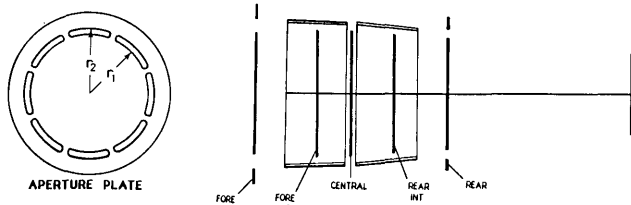


Fig. 2. There are five functionally independent positions for the placement of aperture plates to control ghost images.

has been pointed out that a proper treatment of the ghost image problem involves detailed trade studies which can be complicated and tedious.⁵ We have attempted to develop a systematic approach to the design of aperture plate configurations for ghost image control under various criteria via a detailed analysis of general ghost image behavior in Wolter I systems.

II. Method of Analysis

A FORTRAN computer program that traces a uniform grid of rays through any specified Wolter I system was developed to study the ghost image behavior of Wolter I telescopes. The rays all enter the telescope at a particular angle and are arranged in a square array to simulate uniform illumination of the entrance aperture by a point source at a given field angle. The output of the program is a focal plane spot diagram of the ghost and/or image ray distribution and other ray trace data.

Since there are so many variables in a telescope design which impact ghost image behavior, we per-

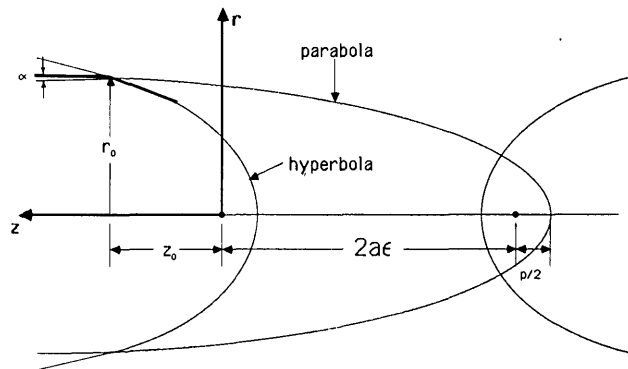


Fig. 3. Coordinate system for the Wolter I telescope used in this paper.

formed our study on a specific nested Wolter I system. Although not perfectly general, parametric analyses of this system have provided a good deal of insight into general ghost image behavior in this class of telescopes. The analyses were performed by exercising the computer program several times, varying one system parameter which impacts ghost image behavior while holding all others fixed.

For the purpose of this study, we developed a Wolter I telescope design consisting of five nested paraboloid-hyperboloid shells with a focal length of 10 m. The innermost shell has a diameter of 600 mm and a grazing angle of 25.8 min of arc at the paraboloid-hyperboloid intersection and was used alone in most of the following analyses. The optical prescription of the telescope is summarized in Table I. The coordinate system from which the tabulated quantities are measured is illustrated in Fig. 3.

Since both vignetting requirements and ghost image requirements place demands on the aperture plate design, we adopted the approach of determining aperture plate sizes by demanding that they unconditionally satisfy the vignetting requirement and then observed the resulting ghost image behavior of the system.

III. General Ghost Image Behavior

The spot diagrams in Fig. 4, generated as aperture plates are sequentially added to a Wolter I system, qualitatively demonstrate the relationship between

Table I. Wolter I Grazing Incidence Telescope Design

	Number of shells		5				
	Nominal focal length		10,000 mm				
	Length of paraboloid		800 mm				
	Length of hyperboloid		800 mm				
	Paraboloid-hyperboloid spacing		50 mm				
Optical prescription data							
Shell	r_0 (mm)	z_0 (mm)	α (radians)	p (mm)	a (mm)	ϵ	
1	600.0000	9981.9675	0.150090E-01	9.0061	4995.4868	1.00090183	
2	525.0000	9986.1997	0.131310E-01	6.8942	4996.5470	1.00069012	
3	450.0000	9989.8647	0.112538E-01	5.0644	4997.4646	1.00050683	
4	375.0000	9992.9638	0.937720E-02	3.5166	4998.2402	1.00035184	
5	300.0000	9995.4980	0.750113E-02	2.2504	4998.8742	1.00022511	

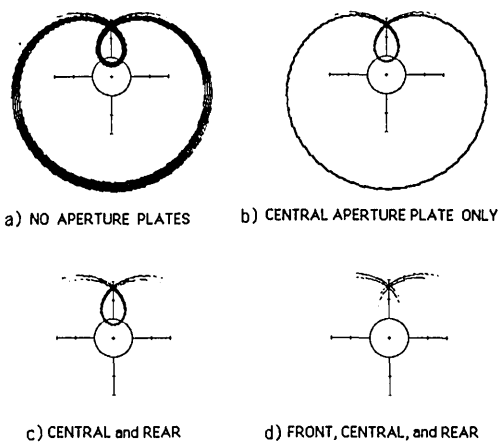


Fig. 4. Ghost image characteristics as aperture plates are sequentially added to a Wolter I telescope.

ghost image characteristics and aperture plate functions. The distribution of singly reflected ghost rays from a point source at a field angle of 40 min of arc when no aperture plates are present in the telescope is shown in Fig. 4(a). The circle centered on the optical axis in the focal plane is 15 min of arc in radius and represents the field within which we would like to exclude all ghost images.

The addition of a central aperture plate which does not introduce any vignetting thins out the ghost ray distribution by blocking many of the ghost rays, as shown in Fig. 4(b). If we now add an aperture plate at the rear of the hyperboloid that satisfies a vignetting requirement, we obtain the ghost image distribution shown in Fig. 4(c). Note that the ghost images furthest from the optical axis have been blocked. Finally, if we add a fore aperture plate in front of the paraboloid which satisfies the same vignetting requirement, the ghost image distribution shown in Fig. 4(d) is produced. This fore aperture has eliminated the ghost images closest to the optical axis.

In this section we examine parametrically the contribution each aperture makes to ghost image control as a function of aperture plate location and the variation of ghost image behavior with telescope grazing angle. A source field angle of 40 min of arc and a vignetting requirement that there shall be no aperture-induced vignetting within 20 min of arc of the optical axis were assumed for all the following examples.

A. Fore Aperture Plate

For an arbitrary vignetting requirement semifield angle ν , the size of the fore aperture as a function of axial position z_{fore} [see Fig. 5(a)] is given by

$$r_{\text{fore2}} = r_{p2} + [(z_{\text{fore}} - z_{p2}) * \tan(\nu)], \quad (1)$$

$$r_{\text{fore1}} = r_{p1} - [(z_{\text{fore}} - z_{p1}) * \tan(\nu)], \quad (2)$$

where (z_{p2}, r_{p2}) and (z_{p1}, r_{p1}) are the axial positions and radii of the front and rear of the paraboloid, respectively.

The fore aperture plate restricts ghost rays from the focal plane within a circle whose diameter increases as

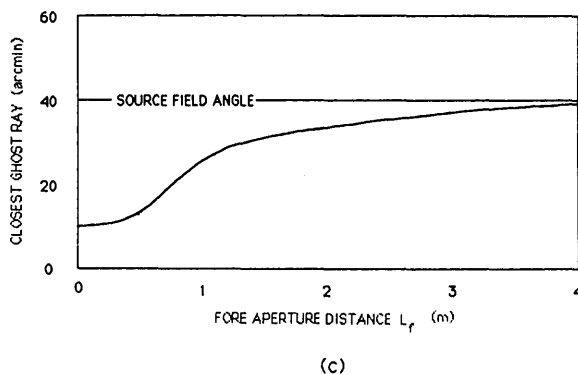
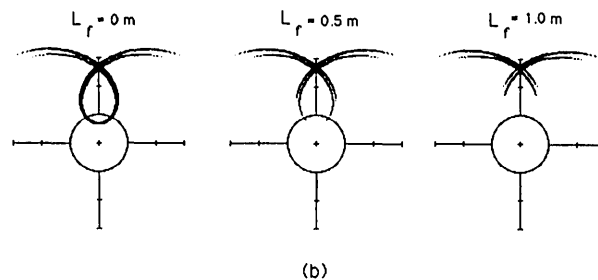
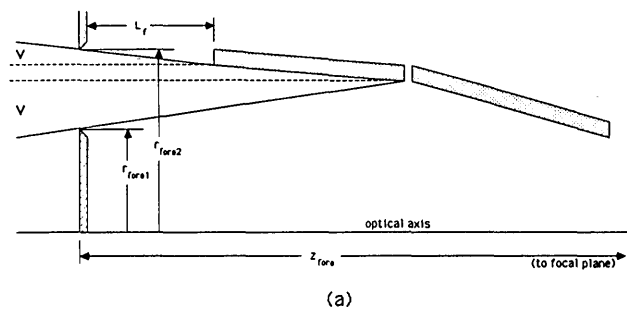


Fig. 5. (a) Placement of the fore aperture plate; (b) ghost images for various positions of the fore aperture plate; (c) closest ghost ray vs axial distance of the fore aperture plate.

the distance between the aperture and the telescope ($L_f = z_{\text{fore}} - z_{p2}$) increases, as demonstrated by the spot diagrams in Fig. 5(b). For this reason, the position of the fore aperture plate is the critical parameter in ghost image control. Figure 5(c) plots the position of the ghost ray closest to axial focus as a function of L_f . Note the asymptotic approach of this position to the source field angle and the inflection point at or near the vignetting requirement half-field angle.

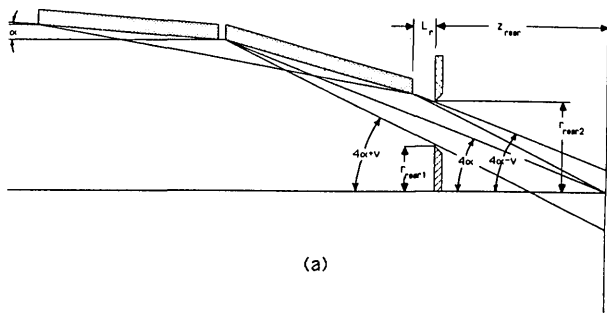
B. Rear Aperture Plate

Similarly, the size of the rear aperture as a function of vignetting requirement ν , nominal grazing angle α , and its axial position z_{rear} [see Fig. 6(a)] is given by

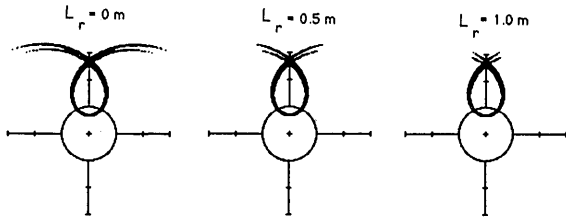
$$r_{\text{rear2}} = r_{h1} - [(z_{h1} - z_{\text{rear}}) * \tan(4\alpha - \nu)], \quad (3)$$

$$r_{\text{rear1}} = r_{h2} - [(z_{h2} - z_{\text{rear}}) * \tan(4\alpha + \nu)], \quad (4)$$

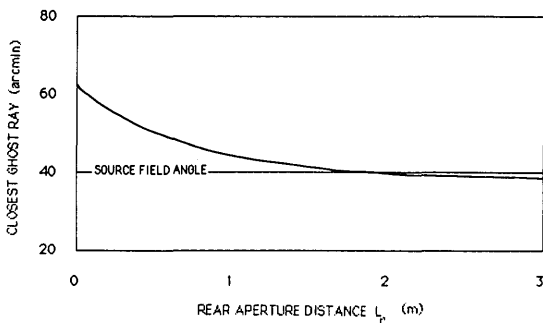
where (z_{h2}, r_{h2}) and (z_{h1}, r_{h1}) are the axial positions and



(a)



(b)



(c)

Fig. 6. (a) Placement of the rear aperture plate; (b) ghost image for various positions of the rear aperture plate; (c) furthest ghost ray vs axial position of the rear aperture plate.

radii of the front and rear of the hyperboloid, respectively.

The rear aperture plate restricts ghost rays from the focal plane outside a circle whose diameter decreases as the distance between the aperture and the telescope ($L_r = z_{h1} - z_{rear}$) increases, as shown in Fig. 6(b). This aperture does not contribute whatsoever to ghost image control near the on-axis focal point. Interestingly, the position of the ghost ray furthest from axial focus actually dips below the source field angle at large values of L_r [Fig. 6(c)]. This implies that, at least for this particular system, ghost images could be completely eliminated from the focal plane with the appropriate choices of L_f and L_r .

C. Central and Intermediate Aperture Plates

The inner radius of the central aperture was chosen such that it lies on the line between the front of the paraboloid and the rear of the hyperboloid:

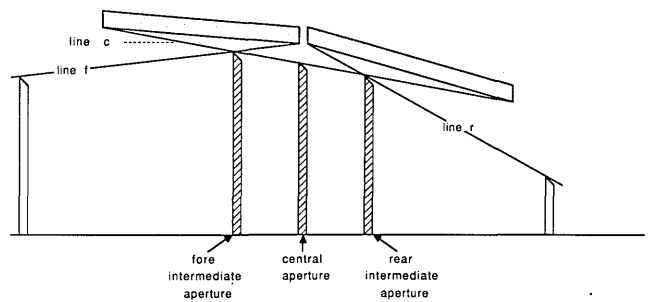


Fig. 7. Location of the central and intermediate aperture plates.

$$r_{cent1} = (m_c * z_{cent}) + b_c, \quad (5)$$

where

$$m_c = (r_{p2} - r_{h1}) / (z_{p2} - z_{h1}),$$

$$b_c = r_{p2} - (m_c * z_{p2})$$

are the slope and intercept of line c in Fig. 7.

The intermediate apertures are also inner radius apertures which lie at the intersection of line c and the lines defining the inner radii of the fore and rear apertures (lines f and r in Fig. 7). At these positions, the fore and rear intermediate apertures do not introduce any additional vignetting. Let (m_f, b_f) and (m_r, b_r) be the (slopes, intercepts) of lines f and r , respectively. The axial positions and radii of the fore (f_{int}) and rear (r_{int}) intermediate aperture plates are given below in terms of the parameters of lines c , f , and r :

$$z_{fint} = (b_f - b_c) / (m_c - m_f), \quad (6)$$

$$r_{fint} = (m_c * z_{fint}) + b_c, \quad (7)$$

$$z_{rint} = (b_r - b_c) / (m_c - m_r), \quad (8)$$

$$r_{rint} = (m_c * z_{rint}) + b_c. \quad (9)$$

One purpose of the central and intermediate aperture plates is to keep any unreflected rays from striking the focal plane. This is accomplished by requiring that they lie along line c . The central aperture, in the absence of the intermediate apertures, serves as a limiting aperture in the sense that the ghost rays (singly reflected from either the paraboloid or the hyperboloid) that come closest to axial focus are those which just graze the fore and central aperture plates. The fore and rear intermediate aperture plates, if included in the system, become limiting apertures for rays singly reflected from the hyperboloid or paraboloid, respectively. The effects on ghost image control by the inclusion of the intermediate aperture plates are demonstrated in Fig. 8. A typical spot diagram from a system containing a central aperture and no intermediate apertures [Fig. 8(a)] has been decomposed into the rays singly reflected from just the primary and secondary [Fig. 8(b)], which are severely truncated by the included fore and rear intermediate aperture [Fig. 8(c)]. Therefore, if the distance to the fore aperture L_f cannot be made arbitrarily large, significant additional ghost image control can be obtained with the inclusion of the intermediate aperture plates.

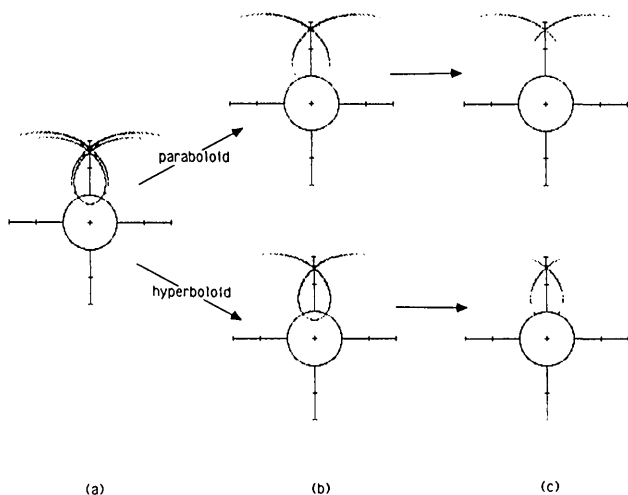


Fig. 8. (a) Typical ghost image consisting of singly reflected rays from a point source at a field angle of 40 min of arc; (b) decomposition of the ghost image into rays singly reflected from the paraboloid or hyperboloid only; (c) dramatic improvement of ghost image behavior with inclusion of intermediate aperture plates.

D. Ghost Image Behavior vs Grazing Angle

The sensitivity of Wolter I systems is determined by the compromise between geometric collecting area and optical efficiency (reflectance), which depends on the telescope's grazing angle. Telescopes may be designed to maximize sensitivity by having many nested shells; the outer shells have larger areas and grazing angles, contributing the bulk of effective area for lower x-ray energies, and the inner shells have smaller areas and grazing angles, contributing the bulk of effective area for higher energies. Grazing angle is a function of telescope diameter and focal length, but focal length for nested systems is constant. Figure 9 shows the dramatic variation of ghost image behavior with grazing angle (via diameter) for the five shells of our nested Wolter I design. The figure stresses the importance of performing ghost image behavior analysis on Wolter I systems, especially when grazing angles are very slight.

IV. Aperture Plate Design

This understanding of general ghost image behavior allows us to develop an aperture plate design capability for Wolter I telescopes which can satisfy specific requirements for vignetting and ghost image control. For example, let us require that (a) there shall be no aperture-induced vignetting for semi-field angles <20 min of arc, and (b) no ghost rays shall fall within 15 min of arc of the on-axis focal point. As discussed in Sec. III, the singly reflected rays which come closest to the on-axis focus are those which just graze the fore and limiting (central or intermediate) apertures. We developed a computer code to determine the focal plane positions of those closest rays as a function of the axial coordinate of the fore aperture plate. The results of an exercise of this code for the five shells of our nested telescope design are plotted in Fig. 10 for configurations in which the central or an intermediate plate is the limiting aperture.

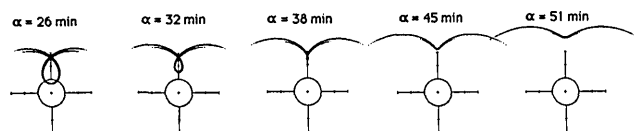


Fig. 9. Ghost images produced by each of the concentric shells of the nested Wolter I telescope described in Table I for an out-of-field source at 40 min of arc. The ghost image problem is much more severe for the smaller grazing angles.

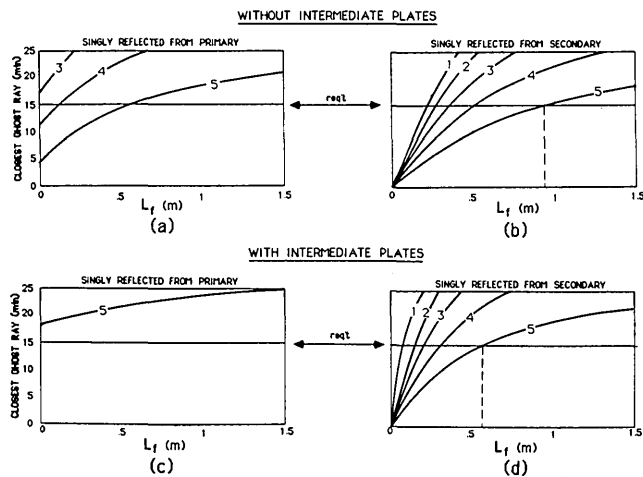


Fig. 10. Position of the closest ghost ray vs fore aperture plate distance L_f for each of the five shells (numbered) of our Wolter I telescope design. The plots are for ghost rays singly reflected from the primary or secondary mirror with the central [(a),(b)] or an intermediate [(c),(d)] plate acting as the limiting aperture.

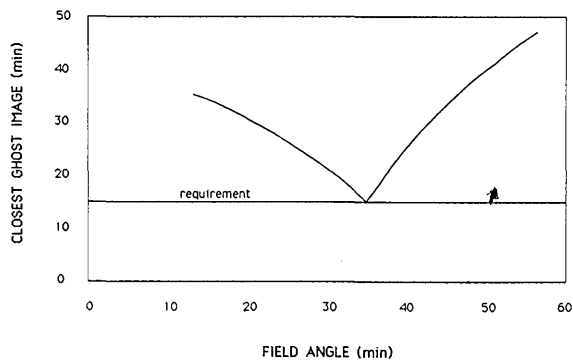


Fig. 11. Position of the closest ghost ray vs source field angle for the fore aperture distance L_f shown in Fig. 10(b) which just satisfies the ghost image requirement.

An aperture plate configuration satisfies the ghost image requirement when the fore aperture is positioned such that it restricts all ghost rays from within the radius specified by the requirement. For this telescope, a fore aperture distance L_f of ~ 90 cm satisfies the ghost image requirement stated above when the central aperture plate is the limiting aperture, as shown in Fig. 10(b). Figure 11 shows that this aperture plate configuration satisfies the ghost image requirement for all source field angles. With the intermediate aperture plates as limiting apertures, an L_f of

only ~ 60 cm is required to satisfy the ghost image requirement shown in Fig. 10(d). Note that regardless of which aperture is limiting, the ghost rays which come closest to axial focus for a given L_f are those singly reflected from the secondary mirror.

V. Alternative Criteria for Ghost Image Control

Physical constraints may exist on a Wolter I system which make it infeasible to place apertures in a configuration that satisfies an absolute ghost image requirement, such as the one described in the previous section. The cusped nature of Fig. 11 implies that, even if an aperture plate design fails to satisfy the ghost image requirement, it would only fail for a narrow range of source field angles. Furthermore, spot diagrams for aperture plate designs which just fail to meet the ghost image requirement indicate that only very few rays actually fall within the radius that the requirement defines. There may be, therefore, other criteria for ghost image control which can be formulated into acceptable ghost image requirements.

One alternative requirement may be stated in terms of allowed relative brightness of the ghost image. For such a requirement, the ratio of the intensity of a ghost image (inside the ghost image requirement radius) from an off-axis point source to the intensity of the on-axis image of the same source is specified to be less than some fraction for all source field angles. With the requirement stated this way, it might be appropriate to include the effects of reflectance on the individual rays. The grazing angles of singly reflected rays are much greater than those of doubly reflected image rays (hence reflectances are much lower), so it is expected that the intensity of the image falling within the ghost image radius might be much less than geometrical considerations alone would predict.

All the foregoing analysis has assumed perfectly aligned optics in the Wolter I system. Some preliminary work indicates that ghost image behavior is extremely sensitive to telescope misalignments.⁶ Aperture plate designs for real systems will have to take into account alignment tolerances when determining the aperture plate configurations which will satisfy an absolute ghost image requirement. These configurations will undoubtedly be more extreme for misaligned optics than for aligned, perhaps so much for some

systems as to make the configurations impractical to implement, requiring the adoption of an alternative ghost image specification.

VI. Summary

We have developed computer codes that allow us to analyze parametrically ghost image behavior as a function of aperture plate location, telescope grazing angle, source field angle, and vignetting requirement semi-field angle. We exercised these codes for a nested telescope design developed for this study. We now have an understanding of the roles aperture plates play in ghost image behavior and of the issues most critical to ghost image control. This understanding permits an aperture plate design capability for the control of ghost images in terms of an absolute ghost image requirement. As an example, we designed an aperture plate configuration for specific system parameters and requirements. For the case where a constraint on a system exists preventing the implementation of an aperture plate configuration satisfying an absolute ghost image requirement, we discussed possible alternative ghost image specifications.

This material was presented as paper 830-38 at the Conference on Grazing Incidence Optics for Astronomical and Laboratory Applications, sponsored by SPIE, the International Society for Optical Engineering, 17-19 Aug. 1987, San Diego, CA.

References

1. H. Wolter, "Spiegelsysteme streifenden Einfalls als abbildende Optiken für Röntgenstrahlen," *Ann. Phys.* **10**, 94 (1952).
2. L. P. Van Speybroeck and R. C. Chase, "Design Parameters of Paraboloid-Hyperboloid Telescopes for X-Ray Astronomy," *Appl. Opt.* **11**, 440 (1972).
3. M. V. Zombeck, G. K. Austin, and D. T. Torgerson, "High Resolution Mirror Assembly (HRMA) Optical Systems Study," Smithsonian Astrophysical Observatory Technical Report SAO-AXAF-80-003, 3-27 (1980).
4. L. P. Van Speybroeck, R. C. Chase, and T. F. Zehnpfennig, "Orthogonal Mirror Telescopes for X-Ray Astronomy," *Appl. Opt.* **10**, 945 (1971).
5. A. Bunner, "CXGT X-Ray Telescope Design Study," Perkin-Elmer Engineering Report ER-526, 107 (1982).
6. P. Young and K. Chisholm, Perkin-Elmer Corp., private communication (1987).